magnetochemistry

MDPI

Supplementary Materials: Self-Assembly and Magnetic Order of Bi-Molecular 2D Spin Lattices of M(II,III) Phthalocyanines on Au(111)

Miloš Baljozović [1,*], Xunshan Liu [2], Olha Popova [3], Jan Girovsky [1], Jan Nowakowski [1], Harald Rossmann [1], Thomas Nijs [3], Mina Moradi [1,4], Fatemeh Mousavi [3], Nicholas C. Plumb [5], Milan Radović [5], Nirmalya Ballav [6], Jan Dreiser [5], Silvio Decurtins [2], Igor A. Pašti [7,8], Natalia V. Skorodumova [8,9], Shi-Xia Liu [2,*] and Thomas A. Jung [1,3,*]

1 Laboratory for Micro- and Nanotechnology, Paul Scherrer Institute, 5232 Villigen-PSI, Switzerland; vedatorsk@gmail.com (J.G.); jan.andrzej.nowakowski@gmail.com (J.N.); h_rossmann@gmx.at (H.R.); minamoradi.1989@gmail.com (M.M.)
2 Department of Chemistry, Biochemistry and Pharmaceutical Sciences, University of Bern, Freiestrasse 3, 3012 Bern, Switzerland; xliu350@zstu.edu.cn (X.L.); Silvio.decurtins@unibe.ch (S.D.)
3 Department of Physics, University of Basel, Klingelbergstrasse 82, 4056 Basel, Switzerland; ollia.popova@gmail.com (O.P.); thomask.nijs@gmail.com (T.N.); fatemeh.mousavi@unibas.ch (F.M.)
4 School of Life Science, University of Applied Sciences and Arts, Northwestern Switzerland, Gründenstrasse 40, 4132 Muttenz, Switzerland
5 Swiss Light Source, Paul Scherrer Institute, 5232 Villigen PSI, Switzerland; nicholas.plumb@psi.ch (N.C.P.); milan.radovic@psi.ch (M.R.); jan.dreiser@psi.ch (J.D.)
6 Department of Chemistry, Indian Institute of Science Education and Research, Pune, Maharashtra 411008, India; nballav@iiserpune.ac.in
7 Faculty of Physical Chemistry, University of Belgrade, Studentski trg 12-16, 11000 Belgrade, Serbia; igor@ffh.bg.ac.rs
8 Department of Materials Science and Engineering, School of Industrial Engineering and Management, KTH—Royal Institute of Technology, Brinellvägen 23, 100 44 Stockholm, Sweden; snv123@kth.se
9 Department of Physics and Astronomy, Uppsala University, Box 516, 751 20 Uppsala, Sweden
* Correspondence: milos.baljozovic@psi.ch (M.B.); shi-xia.liu@unibe.ch (S.-X.L.); thomas.jung@psi.ch (T.A.J.)

1. ARPES Investigation of the possible electronic footprint of the supramolecular 2D lattices in the Au(111) surface state

It is interesting to investigate the changes induced by the 2D-Kondo lattice and the ferrimagnetic ordering into the surface states of the Au(111) substrate. In particular we were interested in looking at the shape of the Fermi surface in proximity to the interface and the cuts along the kx, ky directions by means of Angle Resolved Photoelectron Spectroscopy (ARPES). The samples were prepared at the Surface Science Lab and transferred to the high-resolution photoemission spectroscopy (HRPES) endstation at the SIS beamline of the SLS using a slightly modified vacuum suitcase to accommodate the system's sample holders. Upon cooling down the samples to 10-15 K (this provides the lowest reachable temperature at SIS-HRPES) ARPES data were acquired at the $\bar{\Gamma}$-point along the $\bar{\Gamma}$-$\bar{M}$ direction using circularly polarized light with $h\nu = 76$ eV. We started the experiment from a clean Au(111) serving as a reference (Figure S3b-d) where standard dispersion minimum at -0.45 ± 0.05 eV is observed [63,64] but we were not able to resolve the Rashba splitting of the surface state. The dispersion minimum is determined from the peak in Energy Dispersion Curves (EDC) at the $\bar{\Gamma}$-point (blue line on green curve in Figure S3c). Next, we investigated a purely organic molecular system consisting of metal-free phthalocyanine (2HPc) self-assembled on single-crystalline Au(111) substrates (Figure S3e-g). The surface state of the Au(111) substrate is, similar to other cases where π-conjugated systems were adsorbed on substrates with promoted surface states [65-72], shifted towards the Fermi level, in this case by ~0.20 eV. Moreover, significant spectral/band broadening also occurred, most likely due to the inelastic scattering from the deposited molecules. Further on, we have introduced one of the metal centers by preparing a co-assembly of FeFPc and 2HPc on Au(111). Here, the surface state shifts further up by ~0.05 eV (Figure S3h-j). At the same time, spectral broadening increased even more. At this point, however,

one should not exclude possibility that the broadening occurs as a consequence of molecules interacting with the surface state. When the metal free phthalocyanine is replaced by MnPc (Figure S3k-m), surface state shifts back downwards approximately by 0.15 eV. This is a bit surprising, but could happen if the Mn atoms are supplying some charge to the substrate due to their strong interaction with it [73]. Except for the shifts in the surface state and aforementioned band broadening, we didn't observe any other effects, most probably due to the temperature, which was relatively high in view of the known or expected critical temperatures for magnetic ordering. It is still important to keep these surface state shifts in mind as we model the system or for planning the future experiments.

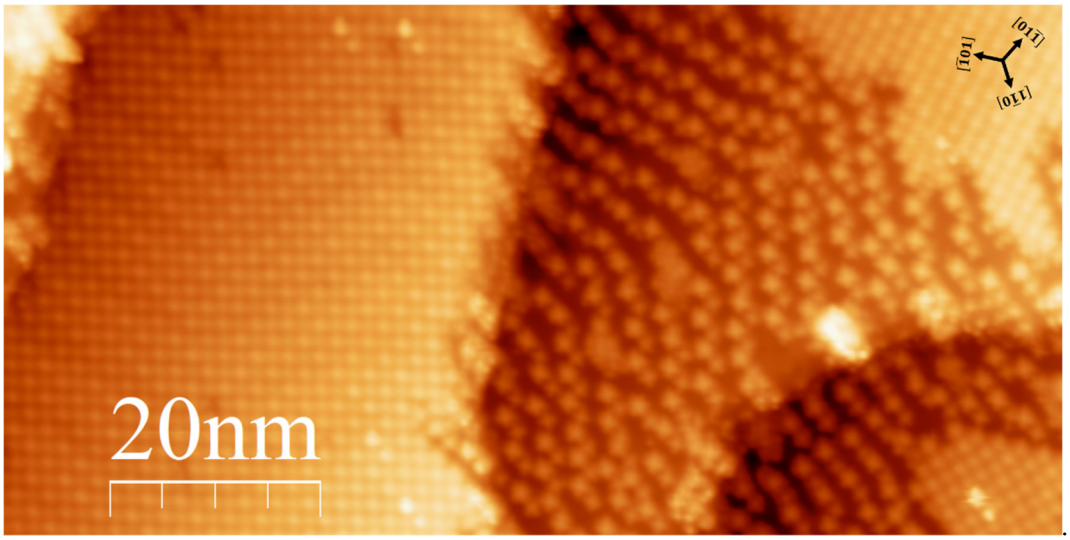

Figure S1. STM micrograph of the assembly of MnPc and FeFPc molecules on Au(111) 50 nm x 100 nm STM micrograph (U = 0.1 V, I = 5 pA) obtained upon subsequent deposition of the molecules. At lower density alternating chains of molecules are formed which follow the fcc/hcp domains of the 22x(sqrt(3))/Au(111) surface reconstruction.

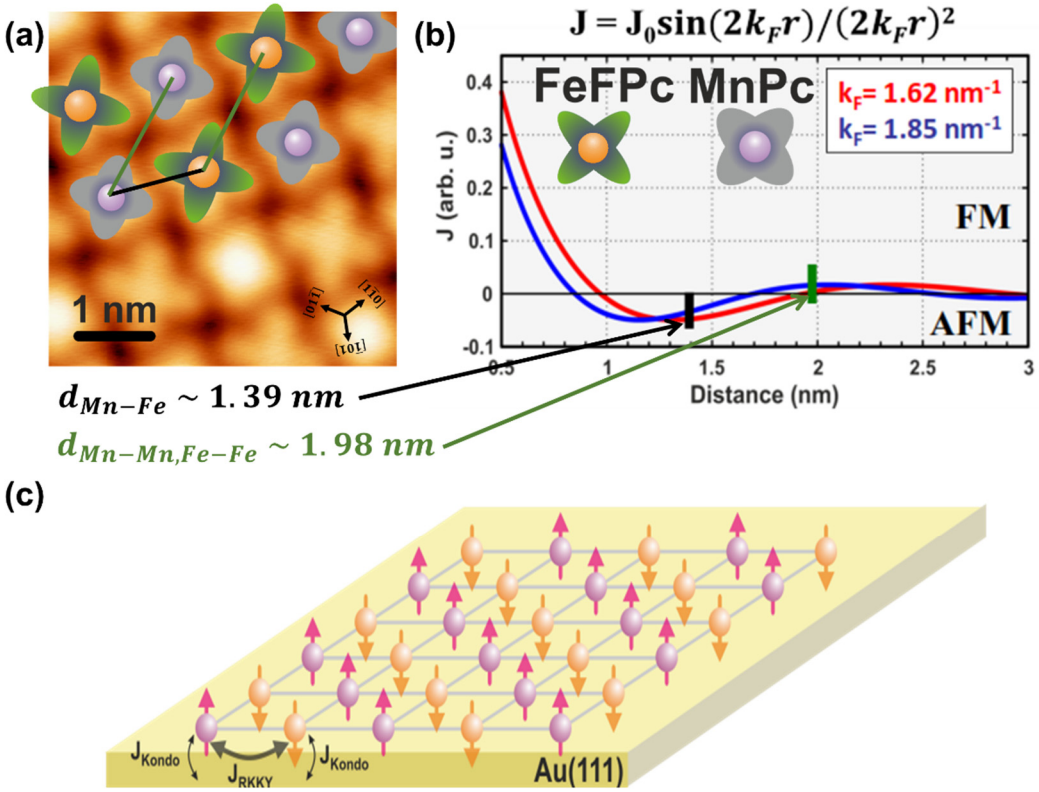

Figure S2. RKKY ordering and formation of 2D ferrimagnet (a) 5 nm x 5 nm STM micrograph (U = -2.2 V, I = 5 pA) from which distances between spin centers are extracted (overlaid with molecular cartoons). (b) Spatial oscillations of the RKKY interaction determined by the two Fermi wave vectors k_F of the Au(111) surface state. Distances between Mn and Fe spins (1.39 nm) fall into AFM coupling regime of RKKY interactions, while distances between Mn and Mn or Fe and Fe centers (1.98 nm) fall into FM coupling regime of RKKY interactions. (c) Illustration of thus formed 2D ferrimagnet. Two distinct sub-lattices of ferromagnetically coupled spin centers (Fe or Mn) are ordered antiferromagnetically to each other, resulting to the ferrimagnetic order due to inequivalent spins of its components, namely Fe and Mn.

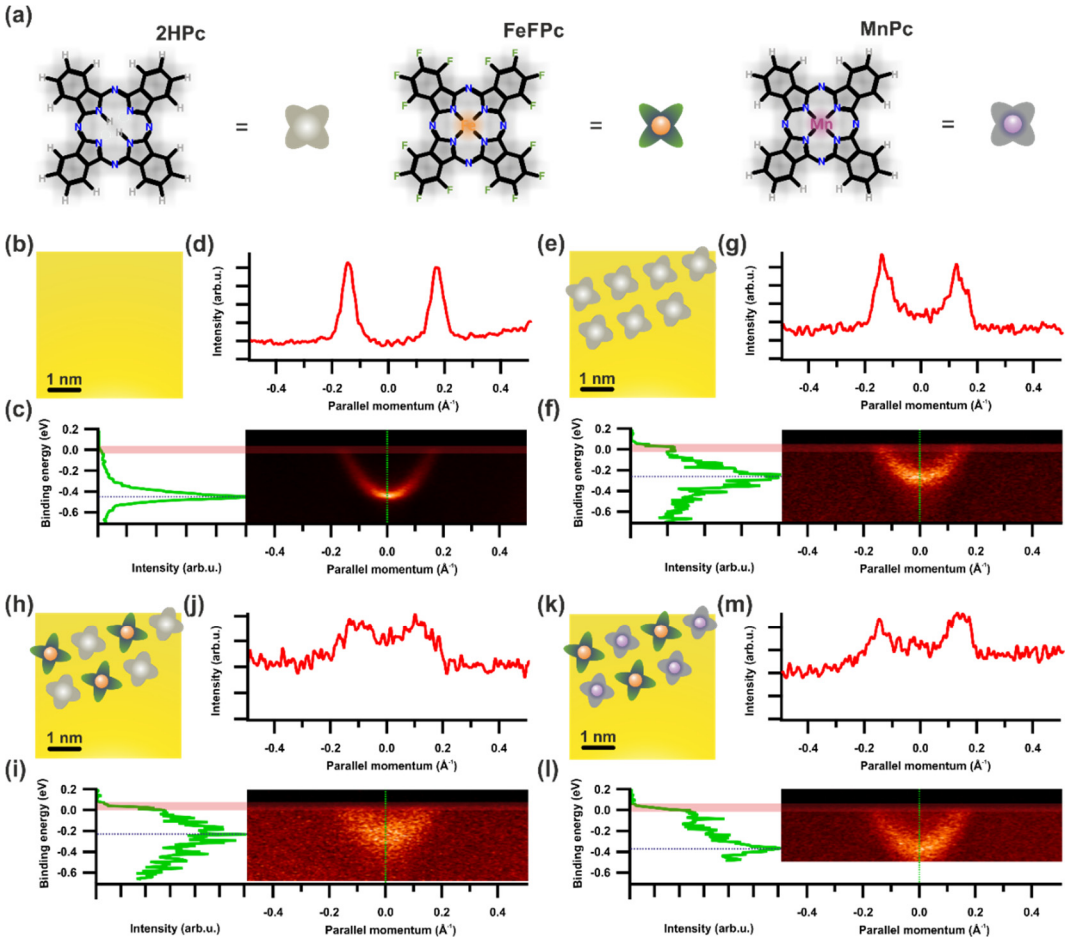

Figure S3. ARPES investigation of the electronic footprint of the supramolecular 2D lattices in the Au(111) surface state (a) molecular structures of the molecules used in ARPES investigations. (b-d) ARPES measurements on clean Au(111) substrate that serve as a reference; (e-g) ARPES measurements on 2HPc covered Au(111) substrate; (h-j) ARPES measurements on 2HPc+FeFPc covered Au(111) substrate; (k-m) ARPES measurements on MnPc+FeFPc covered Au(111) substrate. Green curves in (c,f,i,l) represent EDCs at $\bar{\Gamma}$ point (marked by dashed green line in dispersion maps) and are used to determine bottoms of the band (dashed blue lines). Red curves in (d,g,j,m) represent momentum cuts around Fermi edges summed from the regions marked in red in (c,f,i,l).

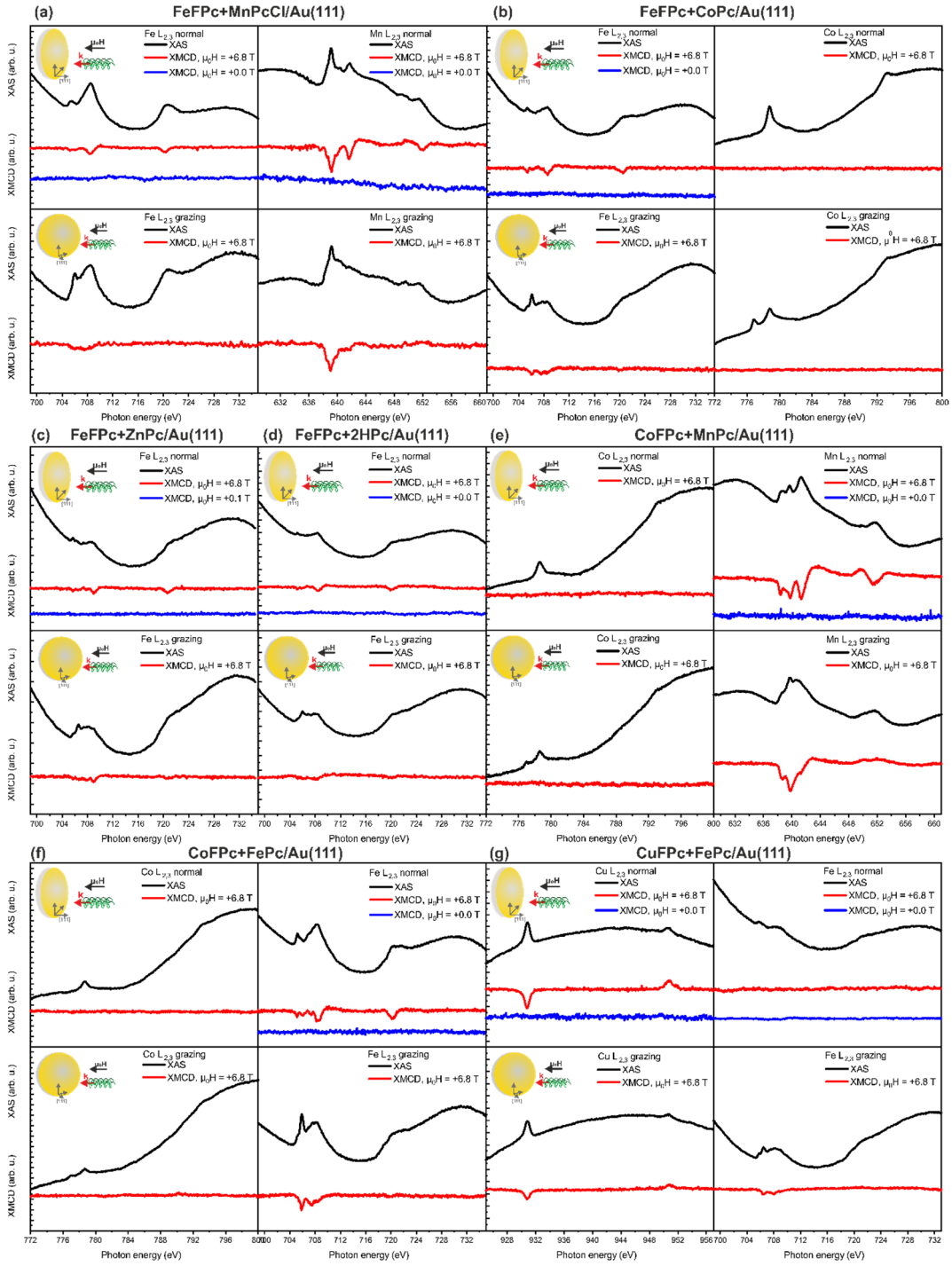

Figure S4. Complete $L_{2,3}$ XAS/XMCD dataset of investigated binary systems on Au(111) (a) FeFPc+MnPcCl; (b) FeFPc+CoPc; (c) FeFPc+ZnPc; (d) FeFPc+2HPc; (e) CoFPc+MnPc; (f) CoFPc+FePc; (g) CuFPc+FePc. XAS (without background subtraction) is plotted in black, XMCD at +6.8 T in red and XMCD at +0.0/0.1 T upon initial magnetization to +6.8 T in blue. Sketch of the experimental set-up of the XAS/XMCD measurements in normal and grazing X-ray incidence is shown as inset. Grazing incidence measurements are used for qualitative assessment of magnetic anisotropy. All experiments have been performed at 2.5 K. No magnetic remanence is observed in normal incidence for any of these systems at 2.5 K.

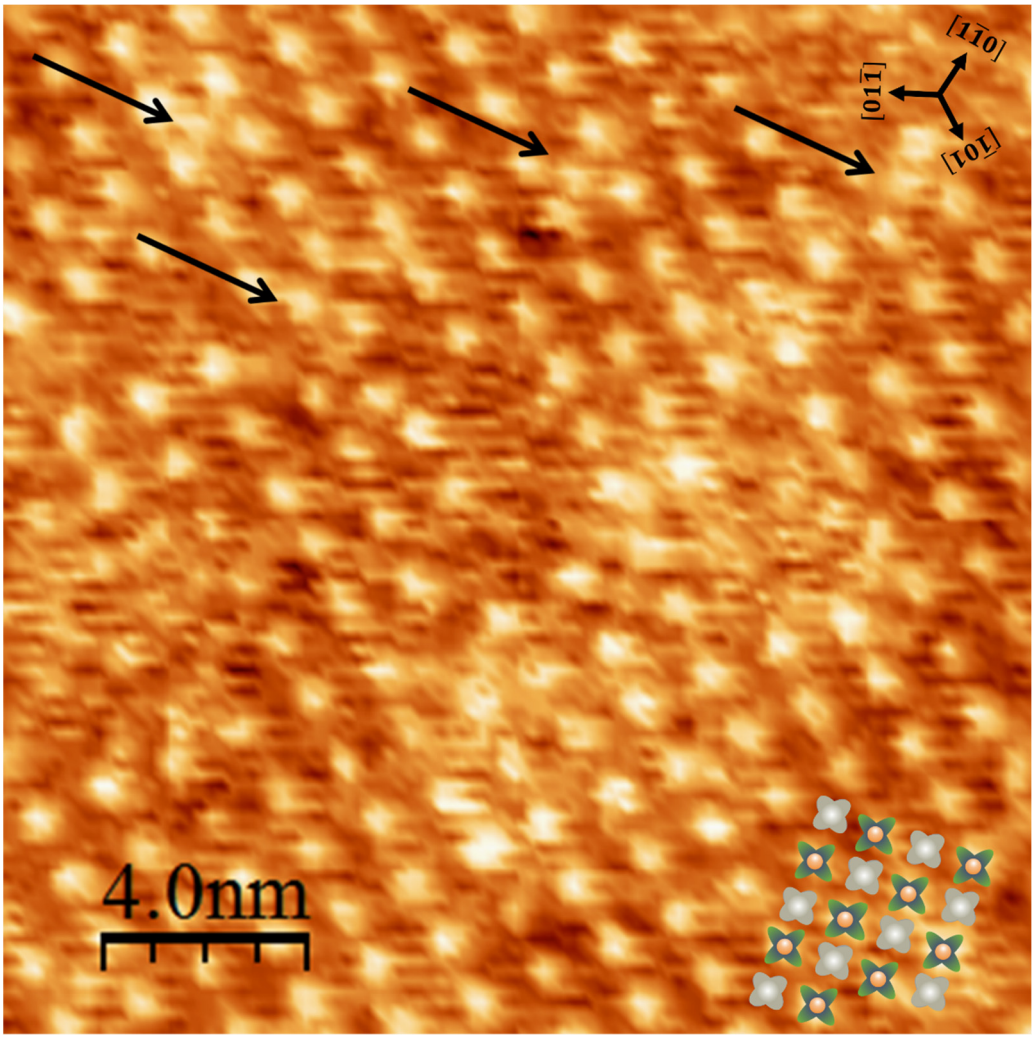

Figure S5. Room temperature STM micrograph of the assembly of 2HPc and FeFPc molecules on Au(111) 20 nm x 20 nm room temperature STM micrograph (U = -0.8 V, I = 10 pA) of a sample where 2HPc and FeFPc molecules co-assembled on Au(111) after their subsequent deposition. Arrows are pointing at the defects where FeFPc replaced 2HPc molecules. Distances in the assembly match nicely with the distances measured in the MnPc+FeFPc assembly.

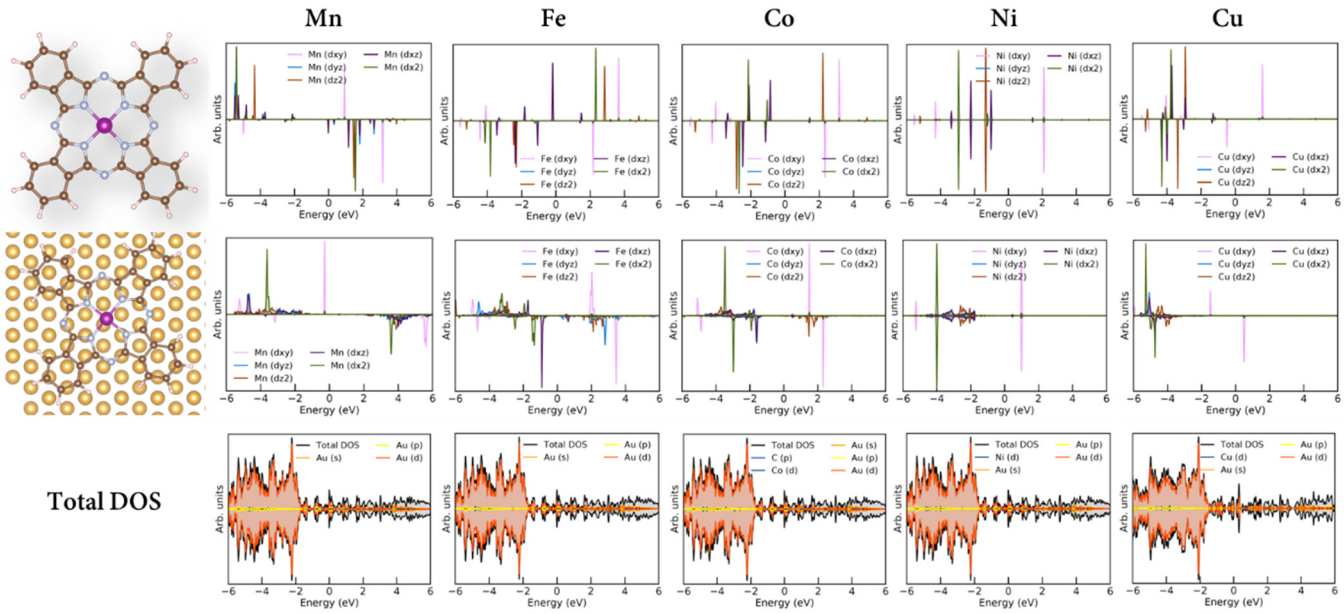

Figure S6. Projected densities of states for isolated and adsorbed molecules. Metal center orbital projected densities of states for Mn, Fe, Co, Ni and Cu in MPc for isolated MPc molecules (top row), adsorbed molecules (middle row) and the total densities of states for MPc molecules adsorbed on Au(111). Fermi level is set to 0 eV.

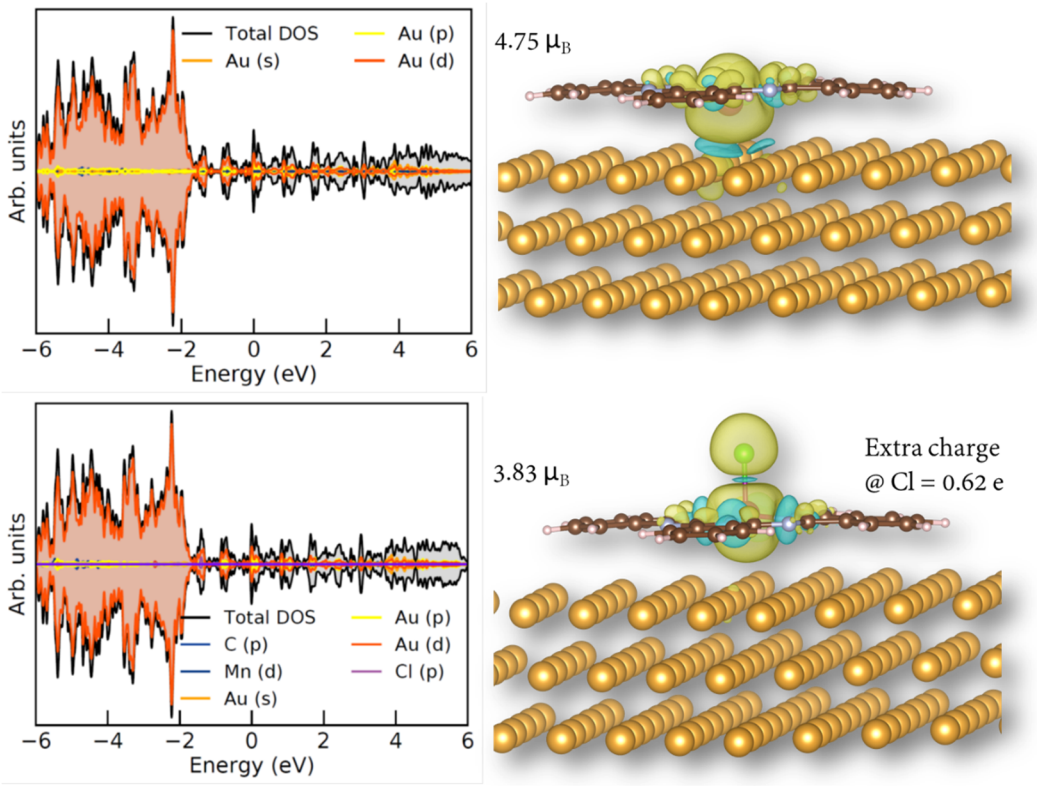

Figure S7. Comparison of MnPc and MnPcCl adsorption on Au(111). Total density of states for MnPc@Au(111) (top left) and MnPcCl@Au(111). Fermi level is set to 0 eV. On the right spin densities are shown (isosurface value $\pm 7\times10^{-4}$ e Å^{-3}), along with the total magnetic moments of the systems and the Bader charge at Cl atom in MnPcCl molecule.